Dynamic equilibria with glass transition heterogeneity and tailorable mechanics in amorphous shape memory polymers

Jingyun Liu[1], Galina Gorbacheva[2], Haibao Lu[1,4], Jiazhi Wang[1,4] and Yong-Qing Fu[3,4]

[1]National Key Laboratory of Science and Technology on Advanced Composites in Special Environments, Harbin Institute of Technology, Harbin 150080, China

[2]Mytishchi Branch of Federal State Budgetary Educational Institution of Higher Education, Bauman Moscow State Technical University, Mytishchi 141005, Russia

[3]Faculty of Engineering and Environment, University of Northumbria, Newcastle upon Tyne, NE1 8ST, UK

[4]E-mail: luhb@hit.edu.cn, wangjiazhi@hit.edu.cn and richard.fu@northumbria.ac.uk

Abstract：Modelling dynamic heterogeneity in amorphous shape memory polymers (SMPs) is a huge challenge due to the complex statistics of strain energy distributions during their thermodynamic relaxations. In this study, based on the dynamic heterogeneity of strain energy distribution, we have considered, for the first time, the influences of different temperature rates and strain rates on strain energy evolution as a dynamic equilibria, rather than a quasi-static problem. We propose a phase transition model incorporated with Gaussian distribution statistics to investigate the dynamic equilibria with glass transition heterogeneity and tailorable mechanics for the amorphous SMPs. The Gaussian distribution statistics is firstly applied to characterize the heterogeneity of strain energy distributions in the amorphous polymers. Phase transition theory is then developed to describe working principles of strain energy evolution, glass transition heterogeneity, thermodynamic relaxation and tailorable

mechanics. Finally, the dynamic equilibria of heterogeneity about the statistics of strain energy distribution are formulated based on the one dimensional Maxwell multi-branch model. The analytical results are compared with the experimental data of epoxy, polyamide and vinylester SMPs reported in literature, and good agreements between them are demonstrated. This study provides a new insight into the dynamic heterogeneity in the mechanics of amorphous SMPs.

Keywords: shape memory polymer; dynamic heterogeneity; glass transition

1. Introduction

Shape memory polymer (SMP) is one of the amazing smart materials which after pre-deformed, can respond to external stimuli and produce mechanical actuations by regaining their permanent shapes [1]. There are various external stimuli to trigger shape recovery, including heat, light, solvent, electric and magnetic fields [2-6]. Shape memory effect (SME) in the SMPs is originated from their intrinsically molecular features of having both hard and soft segments, and can be triggered through either glass transition or melting processes [7]. The unique thermodynamics of SMPs as well as their large deformation strain, low density and tunable properties [8] enable them to have wide-range applications for actuators [9], textile [10], deployable structures [11] and biomedical devices [12-14].

Glass transition is a key factor for generating the SME in amorphous SMPs. In terms of their thermodynamics, heterogeneous molecules in the SMPs preserve various stored strain energies, thus resulting in the multiple glass transitions. SME in the amorphous SMP is originated from the transformation of frozen phases into active

ones, when the frozen phases are heated above their glass transition temperatures [15]. Liu *et al* developed a phase transition model for amorphous SMPs, in which the active and frozen phases were formulated and linked with their shape memory behaviors [16]. Long *et al* proposed another phase transition model to analyze the dynamic behaviors during glass transition of frozen phases in SMPs [17]. Xiao *et al* formulated the constitutive relationship between the relaxation time and fractions of the frozen phases in the SMPs [18]. Guo *et al* studied the constitutive relationship of an amorphous SMP by analyzing the applied stress as a function of the frozen phase fraction [19]. However, these previous studies were focused mainly on the effects of temperature and stress on the glass transition of the homogeneous frozen phases. Whereas effects of strain energy evolution and distributions of the frozen phases within the matrix have never been investigated and understood, even though it is well known that they are strongly associated with the thermodynamic relaxations in the SMPs. When temperature or external load changes, the segments of SMP cannot be immediately rearranged from its original equilibrium state to a new equilibrium state due to its thermodynamic relaxation. Previous models [15-19] generally suggest that the relaxation of segments between two different equilibrium states is consistent and quasi-static. So far, there are few studies on the dynamic heterogeneity and dynamic equilibrium of strain energy distribution during the phase transitions.

In this study, we formulate a constitutive model for the dynamic heterogeneity and strain energy evolution/distribution to explain the tailorable mechanics and stress-strain relationship of the amorphous SMPs. Gaussian distribution statistics [20] of

strain energy is firstly employed to characterize the dynamic heterogeneity of glass transitions. Phase transition theory is then proposed to describe the dynamic equilibria of strain energy evolution/distribution. Furthermore, the constitutive relationships of thermodynamic relaxations and tailorable mechanics have been formulated based on the one-dimensional (1D) Maxwell multi-branch model [21], considering complex statistics of strain energy distribution. Finally, analytical results obtained using our newly developed model are compared with the experimental data of epoxy, polyamide and vinylester SMPs reported in Ref. [22-24] for verifications.

2. Theoretical framework

2.1 Gaussian statistics of energy distribution

SMPs contain a huge number of macromolecules and each of them has conserved different strain energy values. This is often called dynamic heterogeneity, which results in the difficulties to predict the glass transition and relaxation behavior of the SMPs. The initial strain energy distribution of an amorphous polymer is mainly determined by the cooling rate (q_c) during the transition from an equilibrium state to a non-equilibrium state [20]. The distribution probability $P(F)$ of strain energy per mol (F) in the SMP can be expressed using the Gaussian distribution statistics [20],

$$\begin{aligned} P(F) &= \left(2\pi\left\langle\left(\Delta F\right)^2\right\rangle\right)^{-0.5}\exp\left[-\frac{\left(F-c_pT_g\right)^2}{2\left\langle\left(\Delta F\right)^2\right\rangle}\right] \\ &= \left(2\pi c_pRT_g^2\right)^{-0.5}\exp\left[-\frac{\left(F-c_pT_g\right)^2}{2c_pRT_g^2}\right] \end{aligned} \tag{1}$$

where ΔF is the standard energy deviation (per mol) of the Gaussian distribution, c_p is the specific heat, T_g is the glass transition temperature and R (R=8.314 J/mol·K) is the gas constant.

During cooling process, relaxation time (t_{0c}) in the glassy state of a polymer can be expressed using the Arrhenius equation [21], i.e., $t_{0c}=\tau_0 \exp[F_0/(RT)]$. Because there is a certain mount of activation energy to be exchanged with the environment, i.e., a value of c_pT_g at $T=T_g$, the strain energy (F_0) of the SMP can be modified as F_0-c_pT_g [20]. Therefore, the T_g can be derived as [20],

$$T_g = \frac{F_0}{c_p + R\ln(t_{0c}/\tau_0)} \tag{2}$$

where τ_0 is a given constant, and F_0 is the per mol free energy of the SMP in its active state.

Assuming under a constant cooling rate q_c, the relaxation time t_{0c} can be given by,

$$t_{0c} = (T_d - T_e)/q_c \tag{3}$$

where T_d is the temperature for the SMP to be deformed into a temporary shape and T_e is the transition temperature for the SMP in the cooling process.

By substituting equations (2) and (3) into (1), effects of deformation temperature (T_d) and cooling rate (q_c) on the distribution probability of strain energy $P(F)$ can be obtained,

$$\begin{cases} P(F) = \left[2\pi c_p R\left(\dfrac{F_0}{c_p + R\alpha_c}\right)^2\right]^{-0.5} \exp\left[-\dfrac{\left(c_pF + R\alpha_cF - c_pF_0\right)^2}{2c_pRF_0^2}\right] \\ \alpha_c = \ln\left(\dfrac{T_d - T_e}{q_c\tau_0}\right) \end{cases} \tag{4}$$

where α_c is the programming parameter as a function of cooling rate (q_c).

2.2 Dynamic glass transition heterogeneity

The strain energy evolution within the SMPs leads to the dynamic glass transition heterogeneity and various relaxation behaviors. At the relaxation time of t_{0h}, the stored strain energy per mol (F_d) can be expressed by [25],

$$F_{\mathrm{d}} = F_0 - TR\ln\left(t_{0\mathrm{h}}/\tau_0\right) \tag{5}$$

where F_0 is the initial active energy per mol and τ_0 is the initial relaxation time. The item of $t_{0\mathrm{h}}$ refers to the relaxation time for the SMP in the heating process, and has a constitutive relationship with the heating rate (q_{h}),

$$t_{0\mathrm{h}} = (T_{\mathrm{r}} - T_{\mathrm{e}})/q_{\mathrm{h}} \tag{6}$$

where T_{r} is the recovery temperature of SMP from its temporary shape to its permanent shape.

By substituting equation (6) into (5), we can obtain the relationship between stored strain energy (F_{d}) and heating rate (q_{h}),

$$\begin{cases} F_{\mathrm{d}} = F_0 - TR\alpha_{\mathrm{h}} \\ \alpha_{\mathrm{h}} = \ln\left(\dfrac{T_{\mathrm{r}} - T_{\mathrm{e}}}{q_{\mathrm{h}}\tau_0}\right) \end{cases} \tag{7}$$

where α_{h} is the relaxation parameter as a function of heating rate (q_{h}).

According to the equation (7), the stored strain energy (F_{d}) is decreased when the recovery temperature (T_{r}) is increased. Accordingly, the release of stored strain energy can be expressed using a function of the frozen volume fraction (ϕ_{f}), which can be further written using the distribution probability of strain energy ($P(F)$), i.e.,

$$\phi_{\mathrm{f}} = \frac{\varepsilon_{\mathrm{s}}}{\varepsilon_{\mathrm{pre}}} = \int_0^{\infty} P(F)\mathrm{d}F \tag{8}$$

where ε_{s} and $\varepsilon_{\mathrm{pre}}$ are the stored and pre-deformed strains, respectively.

In combination of equations (4) and (8), the frozen volume fraction (ϕ_{f}) in the SMP can be rewritten as,

$$\phi_{\mathrm{f}} = \frac{\varepsilon_{\mathrm{s}}}{\varepsilon_{\mathrm{pre}}} = \int_0^{F_{\mathrm{d}}} \left[2\pi c_{\mathrm{p}} R\left(\frac{F_0}{c_{\mathrm{p}} + R\alpha_{\mathrm{c}}}\right)^2\right]^{-0.5} \exp\left[-\frac{\left(c_{\mathrm{p}}F + R\alpha_{\mathrm{c}}F - c_{\mathrm{p}}F_0\right)^2}{2c_{\mathrm{p}}RF_0^2}\right]\mathrm{d}F \tag{9}$$

To solve the equation (9), the transformation from cartesian integral to polar integral is performed, and following equation is obtained,

$$\begin{cases} \phi_{\mathrm{f}} = \sqrt{1-\exp\left[-\left(\dfrac{R\left(\alpha_{\mathrm{c}}F_0 - c_{\mathrm{p}}\alpha_{\mathrm{h}}T - \alpha_{\mathrm{c}}R\alpha_{\mathrm{h}}T\right)^2}{c_{\mathrm{p}}F_0^2}\right)\right]} \\ \underbrace{\alpha_{\mathrm{c}} = R\ln\left(\dfrac{T_{\mathrm{d}}-T_{\mathrm{e}}}{q_{\mathrm{c}}\tau_0}\right)}_{\text{Programming}}, \quad \underbrace{\alpha_{\mathrm{h}} = R\ln\left(\dfrac{T_{\mathrm{h}}-T_{\mathrm{e}}}{q_{\mathrm{h}}\tau_0}\right)}_{\text{Recoverying}} \end{cases} \tag{10}$$

Based on the equation (10), dynamic glass transition heterogeneity and relaxation behavior can be characterized by the strain energy distribution, which is determined by the thermodynamic history of the SMP. Therefore, it is necessary to investigate the influence of thermodynamic history on the relaxation behavior of SMPs. Based on the Mori-Tanaka equation [26], the SMP is incorporated from the frozen and active phases, where the storage modulus (E) can be expressed as,

$$E = E_{\mathrm{f}}\left(1+\frac{(1-\phi_{\mathrm{f}})(E_{\mathrm{a}}/E_{\mathrm{f}}-1)}{1+\nu\phi_{\mathrm{f}}(E_{\mathrm{a}}/E_{\mathrm{f}}-1)}\right) \tag{11}$$

where E_{a} and E_{f} are the storage moduli of the active and frozen phases, respectively, and ν is the fitting constant.

The storage modulus of the frozen phase has a constitutive relationship with the temperature (T), which can be expressed as [27],

$$\log E_{\mathrm{f}}(T) = \log E(T^{\mathrm{ref}}) - a(T - T^{\mathrm{ref}}) \tag{12}$$

where $E(T^{\mathrm{ref}})$ is the modulus of frozen phase at the reference temperature (T^{ref}), and a is the coefficient of thermal expansion.

Combining equations (10), (11) and (12), the storage modulus (E) of the SMP can be obtained,

$$\begin{cases} E = E_{\mathrm{f}}\left(1+\dfrac{(1-\phi_{\mathrm{f}})(E_{\mathrm{a}}/E_{\mathrm{f}}-1)}{1+\nu\phi_{\mathrm{f}}(E_{\mathrm{a}}/E_{\mathrm{f}}-1)}\right) \\ \log E_{\mathrm{f}}(T) = \log E(T^{\mathrm{ref}}) - a(T-T^{\mathrm{ref}}) \\ \phi_{\mathrm{f}} = \sqrt{1-\exp\left[-\left(\dfrac{R\left(\alpha_{\mathrm{c}}F_0 - c_{\mathrm{p}}\alpha_{\mathrm{h}}T - \alpha_{\mathrm{c}}R\alpha_{\mathrm{h}}T\right)^2}{c_{\mathrm{p}}F_0^2}\right)\right]} \\ \underbrace{\alpha_{\mathrm{c}} = R\ln\left(\dfrac{T_{\mathrm{d}}-T_{\mathrm{e}}}{q_{\mathrm{c}}\tau_0}\right)}_{\text{Programming}}, \quad \underbrace{\alpha_{\mathrm{h}} = R\ln\left(\dfrac{T_{\mathrm{h}}-T_{\mathrm{e}}}{q_{\mathrm{h}}\tau_0}\right)}_{\text{Recoverying}} \end{cases} \tag{13}$$

2.3 Dynamic heterogeneity towards tailorable mechanics

Mechanical performance of the SMP is mainly derived from the stored strain energy, and is strongly linked to the dynamic heterogeneity due to the existence of different characteristics of the frozen phases. Figure 1(a) illustrates the effect of stored strain energy (F_{d}) on the phase transformation. In the amorphous SMPs, the rheological behaviors of frozen and active phases show both viscoelastic and elastic ones, according to the Maxwell multi-branch model [21]. With a stored strain energy (F_{d}) in SMP, a large number of frozen and active phases have been involved into its dynamic transformations. Therefore, thermodynamic phase transition of the SMP can be described by both the frozen and active phases, as shown in Figure 1(b). The active branches can be represented by the elastic springs with a Young's modulus of E_{a0} for the active phases, and the frozen branches can be represented by an elastic spring and a dashpot placed in a series manner for the frozen phases, as reported in Ref. [28].

Because the frozen and active branches are co-existed and activated simultaneously, the strain of each branch in the Maxwell model can be assumed as a constant. Accordingly, the constitutive relationship between the recovery stress (σ) and strain (ε) can be expressed as [19],

$$\sigma = \sum_{i=1}^{m} E_{\mathrm{fi}}(t)\varepsilon + \sum_{j=1}^{n} E_{\mathrm{aj}}\varepsilon \tag{14}$$

where E_{fi} and E_{aj} are the storage moduli of the ith frozen and jth active branches, respectively.

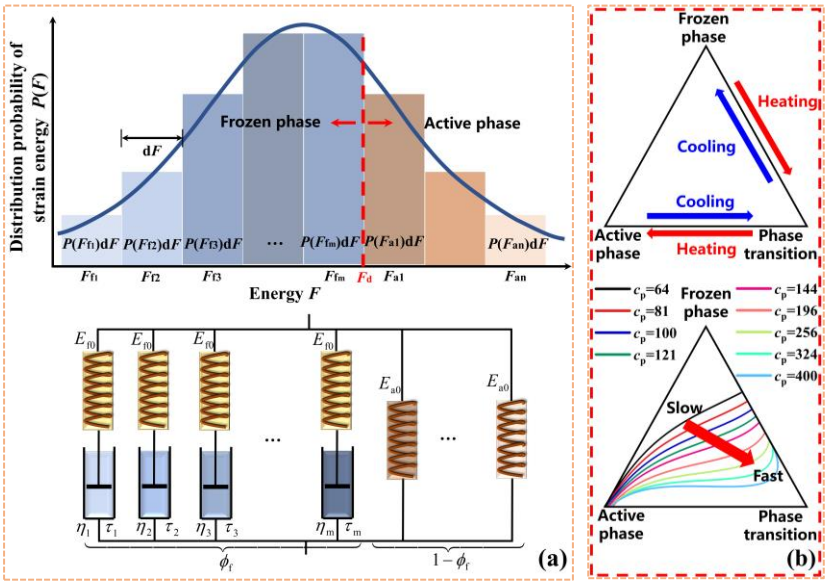

Figure 1. (a) Schematic illustrations of dynamic heterogeneity and rheological behavior of SMP in terms of the stored strain energy and Maxwell multi-branch model, respectively. (b) Schematic illustrations of ternary phase diagram of frozen and active phases at the various specific heats (c_{p}) during heating and cooling processes.

The one-branch Maxwell model can be written as [19],

$$\frac{d\varepsilon}{dt} = \frac{1}{E_{\mathrm{f0}}}\frac{d\sigma_{\mathrm{i}}}{dt} + \frac{\sigma_{\mathrm{i}}}{\eta} \tag{15}$$

where σ_{i} is the recovery stress and η is the viscosity.

Assuming $\varepsilon=\dot{\varepsilon}t$ is the strain under the uniaxial tension (where $\dot{\varepsilon}$ is the strain rate), the recovery stress can be written as,

$$\sigma_{\mathrm{i}} = \varepsilon\frac{\tau(F)}{t}E_{\mathrm{f0}}\left(1-e^{-\frac{t}{\tau(F)}}\right) \tag{16}$$

$$E_{\mathrm{f}}(t)=E_{\mathrm{f0}}\frac{\tau(F_{\mathrm{d}})}{t}\left(1-e^{-\frac{t}{\tau(F)}}\right) \tag{17}$$

where $\tau(F)=\eta/E_{\mathrm{f0}}$ is the relaxion time.

On the other hand, the relaxation time $\tau(F_{\mathrm{d}})$ can be determined by the stored strain energy per mol (F) as follows [20],

$$\tau(F_{\mathrm{d}})=\tau_0\exp\left(\left(F_0-F\right)/T\right) \tag{18}$$

where τ_0 is the relaxation time and F_0 is the initial stored strain energy when $\tau(F_{\mathrm{d}})=\tau_0$.

Substituting equations (1), (17) and (18) into (14), the constitutive relationship of recovery stress and strain of the amorphous SMP under the uniaxial tensile can be obtained,

$$\begin{aligned}\sigma&=\sum_{i=1}^{\mathrm{m}}E_{\mathrm{f}}(t)\varepsilon+\sum_{i=1}^{\mathrm{n}}E_{\mathrm{a0}}\varepsilon=\dot{\varepsilon}t\int_0^{F_{\mathrm{d}}}P(F)E_{\mathrm{f}}(t)dF+\dot{\varepsilon}t\int_{F_{\mathrm{d}}}^{+\infty}P(F)E_{\mathrm{a0}}dF\\&=\dot{\varepsilon}t\int_0^{F_{\mathrm{d}}}P(F)E_{\mathrm{f0}}\frac{\tau}{t}\left(1-e^{-\frac{t}{\tau}}\right)dF+\dot{\varepsilon}t\int_{F_{\mathrm{d}}}^{+\infty}P(F)E_{\mathrm{a0}}dF\\&=E_{\mathrm{f0}}\dot{\varepsilon}\tau_0\left(2\pi c_{\mathrm{p}}RT_{\mathrm{g}}^2\right)^{-0.5}\int_0^{F_{\mathrm{d}}}\exp\left[\frac{F_0-F_{\mathrm{d}}}{RT}-\frac{\left(F-c_{\mathrm{p}}T_{\mathrm{g}}\right)^2}{2c_{\mathrm{p}}RT_{\mathrm{g}}^2}\right]\left(1-e^{-\frac{\varepsilon}{\dot{\varepsilon}\tau_0}\exp\left(\frac{F-F_0}{RT}\right)}\right)dF\\&\quad+\dot{\varepsilon}t\int_{F_{\mathrm{d}}}^{+\infty}P(F)E_{\mathrm{a0}}dF\end{aligned} \tag{19}$$

3. Numerical algorithm and validation on experimental data

3.1 Numerical algorithm

Figure 2 shows the analytical results obtained using equation (4), and the parameters used in calculation are T_{d}=383 K, T_{e}=273 K, τ_0=1 s [22] and F_0=50 kJ/mol [29]. Figure 2(a) presents a cloud chart of distribution probability of strain energy per mol, i.e., $P(F)$ as a function of specific heat. Meanwhile, Figure 2(b) reveals that the distribution probability of strain energy ($P(F)$) in the frozen phase is determined by the specific heat c_{p}, at a given constant of α_{c}=5.39. The maximum distribution

probability of strain energy ($P(F)$) is increased linearly from 3.76×10^{-5} to 6.40×10^{-5} when the specific heat c_p is increased from 64 J/mol·K to 400 J/mol·K. The transition temperature (T_e) of the SMP with a smaller value of specific heat c_p is closer to the ambient temperature, if compared with those with a higher value of specific heat c_p, on the condition that the cooling rate is kept a constant. In the case of fast cooling, the difference between the ambient and transition temperatures of the SMPs is very large, resulting in the frozen transition of active phases within a short relaxation time.

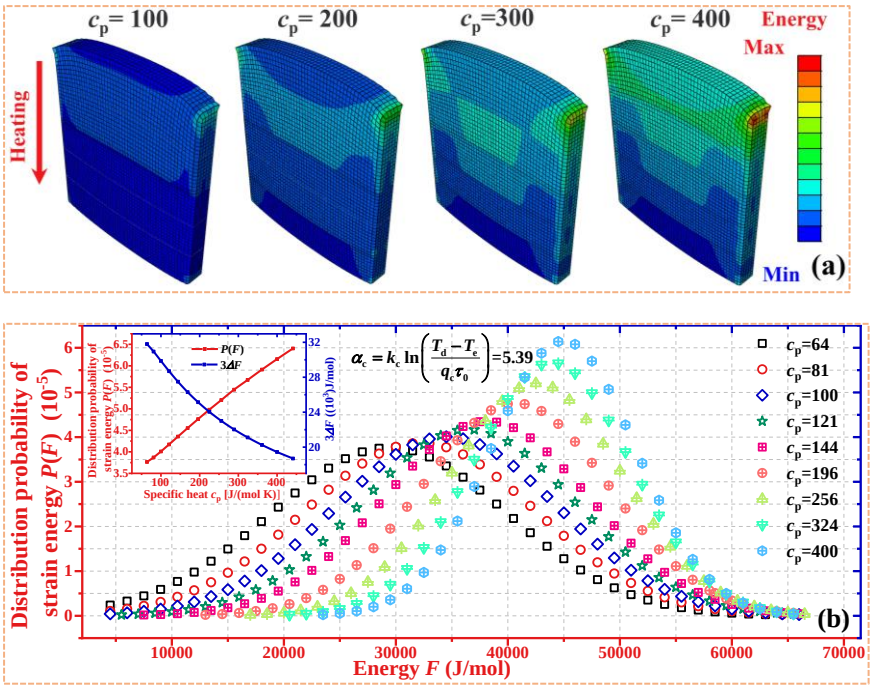

Figure 2. (a) The cloud chart of distribution probability of strain energy $P(F)$ as a function of specific heat, when the specific heat (c_p) is increased from 100 J/(mol·K), 200 J/(mol·K), 300 J/(mol·K) to 400 J/(mol·K). (b) Analytical results of distribution probability of strain energy $P(F)$ as a function of energy, when the specific heat (c_p) is increased from c_p=64 J/(mol·K) to c_p=400 J/(mol·K).

To identify the effects of cooling and heating rates on the frozen volume fraction (ϕ_f) of SMPs, Figure 3 plots the analytical results using the newly proposed model of

equation (13). The parameters used in the calculation using the equation (10) are T_d=T_h=383 K, T_e=273 K, τ_0=1 s [22], F_0=18.5 kJ/mol [29] and c_p=3 J/mol·K [30]. As shown in Figure 3(a), the frozen phase can be effectively transformed into the active ones at a much higher heating rate, when the heating rate is kept a constant of q_h=5 K/min and the T_g value of the SMP is 425 K. These analytical results reveal that the cooling rate (q_c) determines the shift of the transition temperature from the frozen phases into the active ones, and increase of the cooling rate (q_c) decreases the transition temperature.

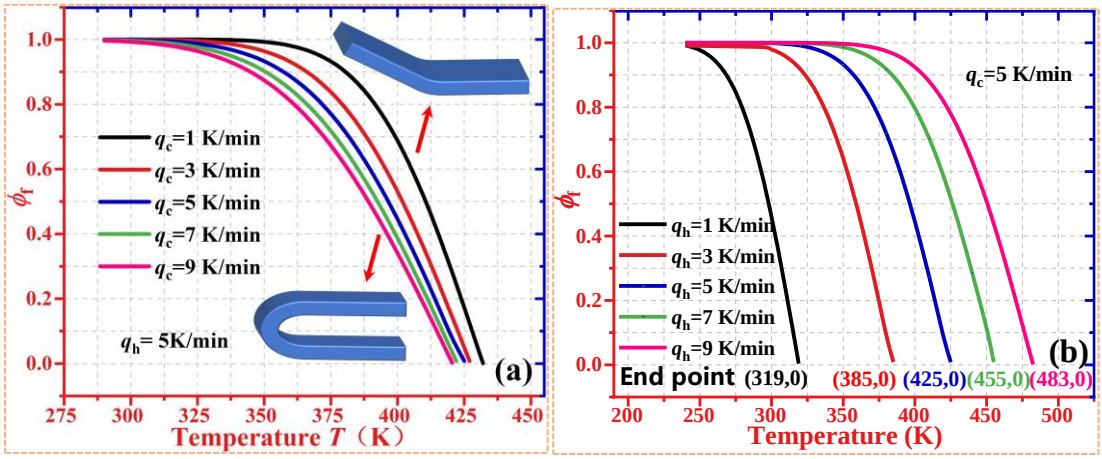

Figure 3. (a) Analytical results of frozen volume fraction (ϕ_f) as a function of temperature at the given cooling rates (q_c) of 1 K/min, 3 K/min, 5 K/min, 7 K/min and 9 K/min. (b) Analytical results of frozen volume fraction (ϕ_f) as a function of temperature at the given heating rates (q_h) of 1 K/min, 3K/min, 5 K/min, 7 K/min and 9 K/min.

Meanwhile, effect of heating rate (q_h) on the frozen volume fraction (ϕ_f) is also investigated using equation (10) and the obtained results are shown in Figure 3(b). The analytical results show that the frozen volume fraction (ϕ_f) is gradually decreased with an increase in the temperature. The values of T_g are 319 K, 385 K, 425K, 455 K and 483 K at various heating rates (q_h) of 1 K/min, 3 K/min, 5 K/min, 7

K/min and 9 K/min, respectively, at a given cooling rate of q_c=5 K/min. It is revealed that a higher cooling rate results in the generation of a much larger stored strain energy and an increased dynamic heterogeneity in the SMP, both of which slow down the transformation of frozen phases into active ones. These analytical results reveal that both the decrease of cooling rate and increase of heating rate are helpful to achieve a high distribution probability of strain energy ($P(F)$) and transformation of frozen phase, resulting in the increased T_g.

Figure 4 shows the analytical results using our newly proposed model (e.g., equation 19) for the SMPs. The parameters used in equation (19) are E_{f0}=978.46 MPa, τ_0=1 s, c_p=0.59166 J/mol·K, T_g=315 K [22], F_0=13 kJ/mol [29] and F_d=164 J/mol, where E_{f0}, T_g are experimental data obtained from Ref. [22], and τ_0, c_p, F_0 and F_d are obtained using the model based on Ref. [29]. Figure 4(a) shows that the recovery stress of SMP is decreased from 36.76 MPa, 31.49 MPa, 26.92 MPa, 23.06 MPa to 19.86 MPa with the temperature increased from 260 K, 270 K, 280 K, 290 K to 300 K, respectively, at a given strain (ε) of 21.5% and strain rate of $\dot{\varepsilon}=3\times10^{-4}$/s. The decrease in recovery stress is mainly due to the increment of molecular mobility and decrement of relaxation time, both of which enable the dynamic heterogeneity and the decrease of stored strain energy with an increment in temperature. On the other hand, Figure 4(b) shows that the recovery stress is gradually increased from 7.83 MPa, 13.93 MPa, 19.86 MPa, 25.38 MPa to 30.35 MPa at a given strain (ε) of 21.5% and ambient temperature of T=300 K, with the strain rate ($\dot{\varepsilon}$) increased from 1×10^{-4}/s, 2×10^{-4}/s, 3×10^{-4}/s, 4×10^{-4}/s to 5×10^{-4}/s. Meanwhile, effects of ambient temperature

and strain rate on the concentrations of frozen and active phases in the SMP have also been illustrated in Figure 4(c). According to the time-temperature superposition theory [31], the increased strain rate is equivalent to the decrement of temperature and increment of the relaxation time, which can lead to an increased dynamic heterogeneity of stored strain energy in the polymer. Therefore, the recovery stress is then increased at the same strain.

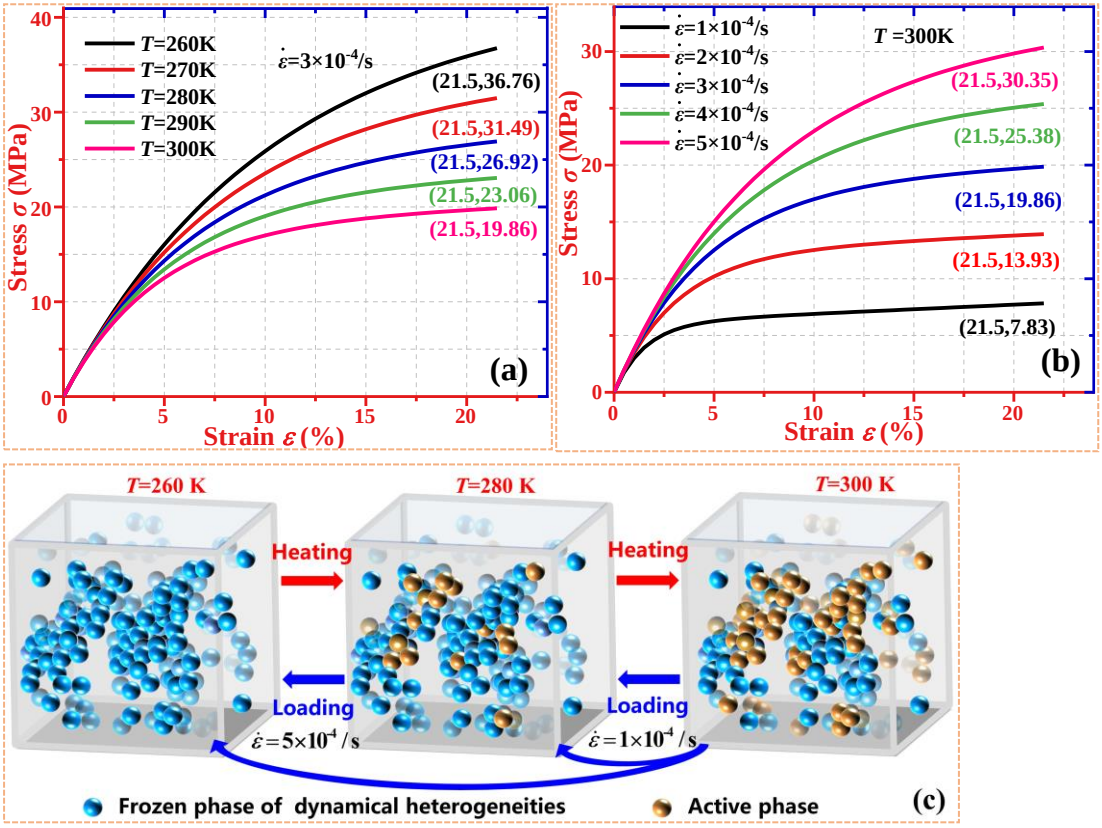

Figure 4. The constitutive stress-stress relationships of amorphous SMP. (a) For the constitutive stress-strain relationship at different ambient temperatures of T=260 K, 270 K, 280 K, 290 K, 300 K. (b) For the constitutive stress-strain relationship at various strain rates of $\dot{\varepsilon}$=1×10^{-4}/s, 2×10^{-4}/s, 3×10^{-4}/s, 4×10^{-4}/s and 5×10^{-4}/s. (c) Aggregation morphology and concentration of frozen and active phases in SMP with respect to heating and loading processes, respectively.

3.2 Validation on experimental data

Experimental data reported in Ref. [22] for the epoxy SMP are used to verify the analytical results generated using our newly proposed model. Based on the frozen volume theory [16], Kim et al [22] analyzed and proved that the volume fraction of frozen phases, storage modulus and strain of epoxy SMP undergoing the shape memory behavior vary with the temperature at different heating rates. The experimental result [22] proved that the microstructure of SMPs cannot be rearranged instantaneously to an equilibrium configuration in response to temperature changes.

Levenberg-Marquardt optimization algorithm is adopted here for all the calculation parameters. It is one of the most widely used a nonlinear least squares algorithms [32], which uses the gradient of data to find their maximum (or minimum) values. Therefore, it simultaneously has the advantages of both the gradient method and Newton method. The key idea of this algorithm is to use the model function to make a linear approximation of the parameter vector, then calculate the partial derivative of each parameter. The derivative term above the second order is ignored, thus the nonlinear least squares problem can be effectively transformed into a linear minimum problem to solve. Table 1 summarizes all the values of the parameters used in the calculations using the equation (10). In Table 1, the heating rates q_h are obtained from Ref. [22], and the value of α_c and α_h are calculated by substituting the cooling rates q_c and the heating rates q_h into equation (10). The values of F_0 and c_p are obtained by the Levenberg-Marquardt optimization algorithm, using equation (10).

Table 1. Values of parameters used in equation (10) for epoxy SMP [22].

q_h (K/min)	F_0 (kJ/mol)	α_c	α_h	c_p J/(mol·K)
3	15.34	4.883	5.394	0.59166
5	14.06		4.883	
7	13.36		4.546	

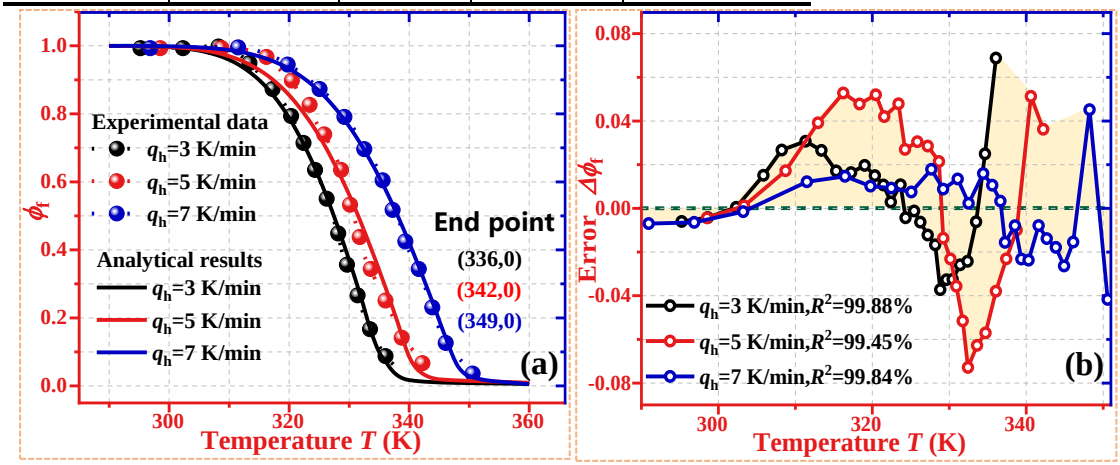

Figure 5. (a) Comparisons of analytical results of equation (10) and experimental data of epoxy SMP [22] for the frozen volume fraction (ϕ_f) as a function of temperature, at various heating rates of q_h=3 K/min, 5 K/min and 7 K/min. (b) Error of analytical and experimental results for frozen volume fraction (ϕ_f).

Figure 5(a) shows the obtained analytical results which reveal that the proposed model can well predict the experimentally obtained results for the epoxy SMP. By increasing the heating rate from 3 K/min, 5 K/min to 7 K/min, the T_g value is increased from 336 K, 342 K to 349 K, where the frozen volume fraction of epoxy SMP is decreased from 1 to 0. With a higher heating rate, a much higher stored strain energy is needed to generate phase transformation from a frozen phase into an active one, resulting into a higher value of distribution probability of strain energy ($P(F)$) and T_g. Furthermore, the correlation index (R^2) between the analytical and experimental results are calculated to be 99.88%, 99.45% and 99.84% for the epoxy

SMP with heating rates of q_h=3K/min, 5 K/min and 7 K/min, respectively, as shown in Figure 5(b). The obtained R^2 data reveal that the analytical results agree well with the experimental ones ($|\Delta\phi_f| \le 0.06$).

To verify the proposed model for the dynamic heterogeneity of strain energy distribution on the thermodynamic behavior of SMPs, equation (13) is applied to predict the thermodynamic properties of the epoxy SMP reported in Ref. [22]. The obtained analytical results are plotted in Figure 6. All the values of parameters used in equation (13) are listed in Table 2, where $E(T^{ref})$=1360 MPa, E_a=3 MPa [22], a=0.0005 [27], v=0.6617 [26] and T^{ref}=305 K. In Table 2, the heating rates q_h are obtained from Ref. [22], and the value of α_c and α_h are calculated by substituting the cooling rates q_c and the heating rates q_h into equation (10). The values of F_0 and c_p are obtained by the Levenberg-Marquardt optimization algorithm, using equation (10).

Table 2. Values of parameters used in equation (13) for epoxy SMP [22].

q_h (K/min)	F_0 (kJ/mol)	α_c	α_h	c_p (J/mol K)
3	12.49	6.245	4.371	0.59166
5	12.50		4.351	
7	12.53		4.267	

As shown in Figure 6(a), with the increase in temperature from 300 K to 361 K, the storage modulus (E) of epoxy SMP is decreased from 978.46 MPa to 2.80 MPa. The T_g is increased from 355 K, 356 K to 361 K, when the heating rate is increased from 3 K/min, 5 K/min to 7 K/min, respectively. Figure 6(a) also shows the experimentally obtained results reported in Ref. [22]. These analytical and experimental results reveal that the dynamic heterogeneity of strain energy distribution in the frozen phase is

highly determined by the heating rate, which enables the transformation from the frozen phase into the active one. At a higher heating rate, a higher value of distribution probability of strain energy ($P(F)$) is achieved according to the equation (13), resulting in a higher dynamic heterogeneity and T_g. Therefore, the relaxation behavior is delayed until at a much higher temperature, and the relaxation time is also increased accordingly. Moreover, the divergences between the analytical and experimental results are calculated based on their correlation index (R^2), and the values are 99.74%, 99.79% and 99.59% for the heating rates of 3 K/min, 5 K/min and 7 K/min, respectively, as shown in Figure 6(b). These results indicate that good agreements between the analytical and experimental results have been obtained, where the error ratio is limited to ±5%.

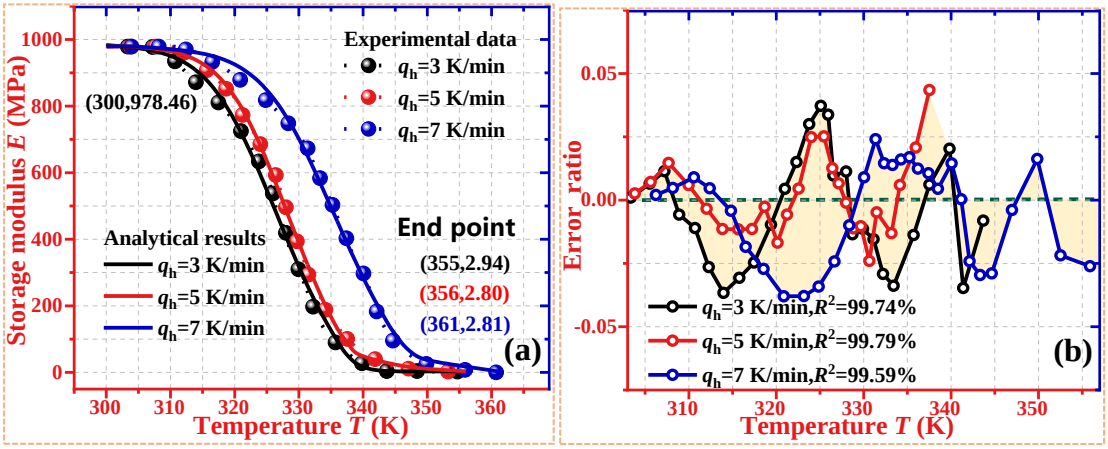

Figure 6. Comparisons between analytical results using equation (13) and experimental data for the epoxy SMP [22]. (a) Storage modulus as a function of temperature, at various heating rates of 3 K/min, 5 K/min and 7 K/min. (b) Divergences of the analytical and experimental results.

Experimental data reported in Ref. [23] for the polyamide SMP are used to verify the analytical results generated from the proposed model using the equation (19). All the parameters used in the calculations are listed as follows: E_{f0}=3500 MPa, E_{a0}=3

MPa, T_g=339 K [23], τ_0=1 s, F_0=20.48 kJ/mol and c_p=2.904 J/mol·K [29], where E_{f0}, E_{a0}, T_g are experimental data from Ref. [23], and τ_0, F_0 and c_p are obtained using the equation (19) and Ref. [29]. As shown in Figure 7(a), the analytical results are in good agreements with the experimental data [23] of the polyamide SMPs. From both the analytical and experimental results, the recovery stress is decreased from 86.79 MPa, 75.09 MPa, 71.46 MPa, 67.08 MPa to 60.71 MPa with an increase in the temperature (T) from 277 K, 294 K, 303 K, 313 K to 323 K, at the same strain of ε=20% and strain rate of $\dot{\varepsilon}$=3.3×10^{-4}/s. Meanwhile, the correlation index of R^2 between the analytical and experimental results are 99.18%, 98.40%, 97.45%, 95.96% and 95.13% at T=277 K, 294 K, 303 K, 313 K and 323 K, respectively, as shown in Figure 7 (b).

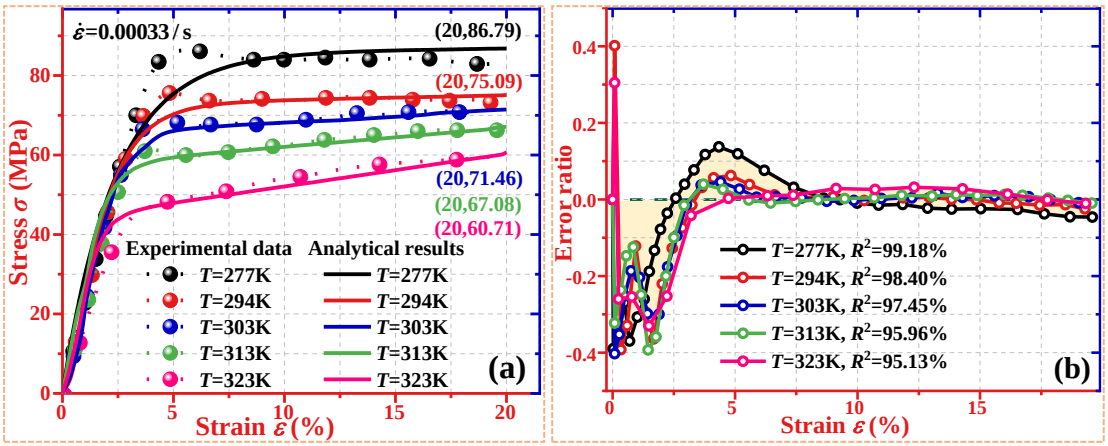

Figure 7. Comparisons between analytical results using equation (19) and experimental data for polyamide SMPs [23]. (a) For the stress-strain curves of polyamide SMPs at different ambient temperatures of T=277 K, 294 K, 303 K, 313 K and 323 K, respectively, at the same strain of ε=20% and strain rate of $\dot{\varepsilon}$=3.3×10^{-4}/s. (b) Error ratio of recovery stress.

To further verify the model, analytical results of recovery stress as a function of strain obtained using equation (19) for the vinylester SMP reported in Ref. [24] are obtained and plotted in Figure 8(a), which have been compared with the experimental

data at various strain rates ($\dot{\varepsilon}$) of 1×10^{-4}/s, 1×10^{-3}/s, 1×10^{-2}/s and 1/s. The parameters used in calculations using equation (19) are listed as follows: E_{f0}=492.24 MPa, E_{a0}=3 MPa, T_g =400 K [24], τ_0=1 s, F_0=25.82 kJ/mol and c_p=3.02 J/mol·K [29], where E_{f0}, E_{a0}, T_g are experimental data from Ref. [24], and τ_0, F_0 and c_p are obtained using the equation (19) and Ref. [29]. Both the analytical and experimental results in Figure 8(a) show that the recovery stress is gradually increased from 62.6 MPa, 72.34 MPa, 83.29 MPa to 110.35 MPa, with an increase in the strain rate ($\dot{\varepsilon}$) from 1×10^{-4}/s, 1×10^{-3}/s, 1×10^{-2}/s to 1/s, at the same strain of ε=5%. It is revealed that the analytical results agree well with the experimental data. According to both the analytical results and experimental data, with the increase of strain rate, the vinylester SMP has a longer relaxation time, a higher dynamic heterogeneity, and thus a higher recovery stress. Meanwhile, the correlation index (R^2) between the analytical and experimental results are calculated as 96.73%, 96.90%, 98.15% and 99.62% for the vinylester SMP [24] at $\dot{\varepsilon}$ of 1×10^{-4}/s, 1×10^{-3}/s, 1×10^{-2}/s and 1/s, respectively, as shown in Figure 8(b).

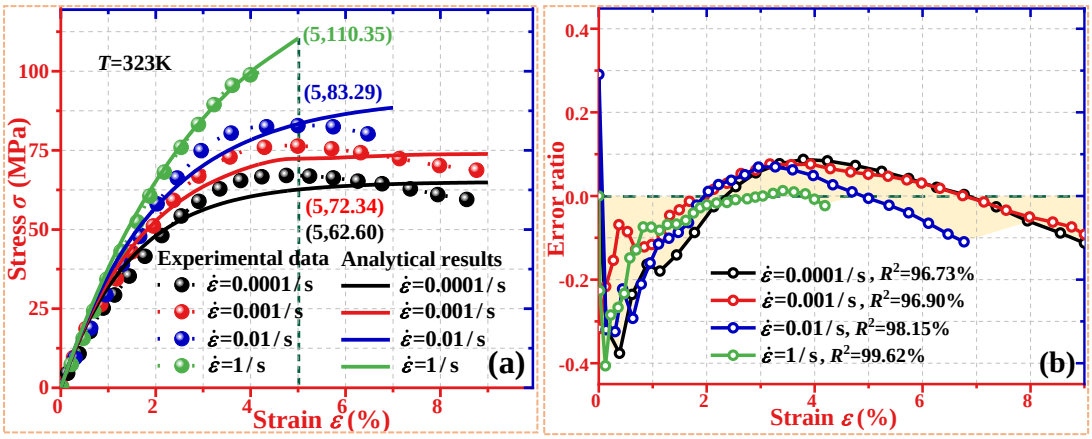

Figure 8. Comparisons between analytical results using equation (19) and experimental data [24] of stress-strain curves of vinylester SMP at T=323 K. (a) For the stress-strain curves of vinylester SMP at $\dot{\varepsilon}$=1×10^{-4}/s, 1×10^{-3}/s, 1×10^{-2}/s and 1/s, respectively. (b) Error ratio of recovery stress.

4. Conclusion

To explore the dynamic principle in SME, we propose an analytical model to describe the glass transition heterogeneity and relaxation behavior of the SMP. The dynamic SME in the SMP is fundamentally originated from the stored strain energy, of which its energy distribution determines the shape recovery and relaxation behaviors. Gaussian distribution statistics is firstly used to describe the dynamic heterogeneity and strain energy distribution, which play essential roles to determine the transformation of frozen phase in SMP. Phase transition theory is then proposed to investigate the transformation from a frozen phase into an active one, to formulate the constitutive relationship between dynamic heterogeneity and strain energy distribution. Finally, the dynamic equilibria of heterogeneity have been formulated based on the Maxwell multi-branch model, to explore the working principle of dynamic heterogeneity in relaxation behavior and tailorable mechanics of SMP. The analytical results obtained from the epoxy, polyamide and vinylester SMPs are compared with the experimental data reported in the literature, and good agreements between them were obtained. The dynamic equilibria are established by introducing the dynamic heterogeneity of strain energy distribution, which considers the effects of different thermal histories (heating rate of q_h and cooling rate of q_c) and different strain rate on the dynamic heterogeneity of strain energy and glass transition can explain the thermodynamic and thermomechanical behaviors of the SMPs. This study provides a fundamental model strategy to explore the working principle of dynamic heterogeneity in the amorphous SMP, of which the SME is determined by the

thermodynamic history, undergoing multiple glass transitions and relaxation behaviors simultaneously.

Acknowledgements

This work was financially supported by the National Natural Science Foundation of China (NSFC) under Grant No. 11725208 and 12172107, International Exchange Grant (IEC/NSFC/201078) through Royal Society and NFSC.

References

[1] Fang Y, Ni Y L, Leo S Y, Taylor C, Basile V and Jiang P 2015 Reconfigurable photonic crystals enabled by pressure-responsive shape-memory polymers *Nat. Commun.* **6** 1–8

[2] Lu H B, Liu Y J, Leng J S and Du S Y 2009 Qualitative separation of the effect of the solubility parameter on the recovery behavior of shape-memory polymer *Smart Mater. Struct*. **18** 085003

[3] Yang B, Huang W M, Li C, Lee C M and Li L 2004 On the effects of moisture in a polyurethane shape memory polymer *Smart Mater. Struct*. **3** 191–5

[4] Lu H B, Liu Y J, Leng J S and Du S Y 2010 Qualitative separation of the physical swelling effect on the recovery behavior of shape memory polymer *Eur. Polym. J.* **46** 1908–14

[5] Ji S B, Fan F Q, Sun C X, Yu Y and Xu H P 2017 Visible light-induced plasticity of shape memory polymers *ACS Appl. Mater. Inter*.**9** 3169–75

[6] Cho J W, Kim J W, Jung Y C and Goo N S 2005 Electroactive shape-memory polyurethane composites incorporating carbon nanotubes *Macromol. Rapid Commun*. **26** 412–6

[7] Meng H and Li G Q 2013 A review of stimuli-responsive shape memory polymer composites *Polymer* **54** 2199–221

[8] Meng Q and Hu J 2009 A review of shape memory polymer composites and blends *Composites: Part* A **40** 1661-72

[9] Zhang Y F, Zhang N B, Hingorani H, Ding N Y, Wang D, Yuan C, Zhang B, Gu G Y and Ge Q 2019 Fast-response, stiffness-tunable soft actuator by hybrid multimaterial 3D printing *Adv. Funct. Mater.* **29** 1806698

[10] Vili Y Y F C 2007 Investigating smart textiles based on shape memory materials *Text. Res. J.* **77** 290–300

[11] Santo L, Quadrini F, Squeo E A, Dolce F, Mascetti G, Bertolotto D, Villadei W, Ganga P L and Zolesi V 2012 Behavior of shape memory epoxy foams in microgravity: experimental results of STS-134 mission *Microgravity Sci. Technol.* **24** 287–96

[12] Ortega J M, Hartman J, Rodriguez J N and Maitland D J 2013 Virtual treatment of basilar aneurysms using shape memory polymer foam *Ann. Biomed. Eng.* **41** 725–43

[13] Delaey J, Dubruel P and Van Vlierberghe S 2020 Shape-memory polymers for biomedical applications *Adv. Funct. Mater.* **30** 1909047

[14] Lendlein A and Langer R 2002 Biodegradable, elastic shape-memory polymers for potential biomedical applications *Science* **296** 1673–6

[15] Ge Q, Yu K, Ding Y and Qi H J 2012 Prediction of temperature-dependent free recovery

behaviours of amorphous shape memory polymers *Soft Matter* **8** 11098–105

[16] Liu Y P, Gall K, Dunn M L, Greenberg A R and Diani J 2006 Thermomechanics of shape memory polymers: uniaxial experiments and constitutive modeling *Int. J. Plast.* **22** 279–313

[17] Long K N, Dunn M L and Qi H J 2010 Mechanics of soft active materials with phase evolution *Int. J. Plast.* **26** 603–16

[18] Xiao R, Choi J, Lakhera N, Yakacki C M, Frick C P and Nguyen T D 2013 Modeling the glass transition of amorphous networks for shape-memory behavior *J. Mech. Phys. Solids* **61** 1613–35

[19] Guo X, Liu L, Liu Y, Zhou B and Leng J S 2014 Constitutive model for a stress- and thermal-induced phase transition in a shape memory polymer *Smart. Mater. Struct.* **23** 105019

[20] Dyre J C 1987 Master-equation approach to the glass-transition *Phys. Rev. Lett.* **58** 792-5

[21] Treloar L R G 2005 *The physics of rubber elasticity* (Oxford, NY: Oxford University Press)

[22] Kim J, Jeon S Y, Hong S, An Y, Park H and Yu W R 2021 Three-dimensional constitutive model for shape-memory polymers considering temperature-rate dependent behavior *Smart. Mater. Struct.* **30** 035030

[23] Le Gac P Y, Arhant M, Le Gall M and Davies P 2017 Yield stress changes induced by water in polyamide 6: characterization and modeling *Polym. Degrad. Stabil.* **137** 272–280

[24] Plaseied A and Fatemi A 2008 Strain Rate and Temperature Effects on Tensile Properties

and Their Representation in Deformation Modeling of Vinyl Ester Polymer *Int. J. Polym. Mater.* **57** 463–79

[25] Dyre J C 1995 Energy master equation-a low temperature approximation to basslers random-walk model *Phys. Rev. B* **51** 12276-94

[26] Weng G J 1984 Some elastic properties of reinforced solids, with special reference to isotropic ones containing spherical inclusions *Int. J. Eng. Sci.* **22** 845

[27] Arruda E M and Boyce M C 1993 Evolution of plastic anisotropy in amorphous polymers during finite straining *Int. J. Plast.* **9** 697–720

[28] Yu K, Xie T, Leng J S, Ding Y F and Qi H J 2012 Mechanisms of multi-shape memory effects and associated energy release in shape memory polymers *Soft matter* **8** 5687-95

[29] Adam G and Gibbs J H 1965 On the temperature dependence of cooperative relaxation properties in glass-forming liquids *J. Chem. Phys.* **43** 139–46

[30] Wunderlich B 1960 Study of the change in specific heat of monomeric and polymeric glasses during the glass transition *J. Phys. Chem.* **64** 1052–6

[31] Williams M L, Landel R F and Ferry J D 1955 The temperature dependence of relaxation mechanisms in amorphous polymers and other glass-forming liquids *J. Am. Chem. Soc.* **77** 3701–7

[32] Fan J Y and Pan J Y 2009 A note on the Levenberg–Marquardt parameter *App. Math. Comput.* **207** 351–9